Journal of ELECTRONIC MATERIALS, Vol. 39, No. 9, 2010
DOI: 10.1007/s11664-010-1312-3

Physical Properties of Single-Crystalline $Ba_8Ni_{3.5}Ge_{42.1}\square_{0.4}$

L.T.K. NGUYEN,[1,2,3,4] U. AYDEMIR,[3] M. BAITINGER,[3] J. CUSTERS,[1] A. HAGHIGHIRAD,[2] R. HÖFLER,[1] K.D. LUTHER,[2] F. RITTER,[2] YU. GRIN,[3] W. ASSMUS,[2] and S. PASCHEN[1]

1.—Institute of Solid State Physics, Vienna University of Technology, Wiedner Hauptstr. 8-10, 1040 Vienna, Austria. 2.—Institute of Physics, Goethe-University Frankfurt am Main, Max-von-Laue-Str.1, 60431 Frankfurt am Main, Germany. 3.—Max-Planck-Institut für Chemische Physik fester Stoffe, Nöthnitzer Str. 40, 01187 Dresden, Germany. 4.—e-mail: lien@ifp.tuwien.ac.at

Clathrates are candidate materials for thermoelectric applications because of a number of unique properties. The clathrate I phases in the Ba-Ni-Ge ternary system allow controlled variation of the charge carrier concentration by adjusting the Ni content. Depending on the Ni content, the physical properties vary from metal-like to insulator-like and show a transition from *p*-type to *n*-type conduction. Here we present first results on the characterization of millimeter-sized single crystals grown by the Bridgman technique. Single crystals with a composition of $Ba_8Ni_{3.5}Ge_{42.1}\square_{0.4}$ show metallic behavior ($d\rho/dT > 0$) albeit with high resistivity at room temperature [ρ (300 K) = 1 mΩ cm]. The charge carrier concentration at 300 K, as determined from Hall-effect measurements, is 2.3 e^-/unit cell. The dimensionless thermoelectric figure of merit estimated at 680 K is $ZT \approx 0.2$.

Key words: Clathrates, thermoelectric material, intermetallic compound, nickel

INTRODUCTION

Intermetallic clathrates are currently under investigation because of their potential as thermoelectric materials. Their crystal structures consist of a covalently bonded framework of mainly group 13 and group 14 elements with large polyhedral cages, which can be filled by electropositive metal atoms. In type I clathrates, each unit cell contains two small 20-atom cages, X_{20}, and six large 24-atom cages, X_{24} (Fig. 1).

The low lattice thermal conductivity κ_l of clathrates is explained by the interaction of localized vibration modes of the encapsulated metal atoms ("guest" atoms) with heat-carrying phonons.[1,2] In addition, for a high thermoelectric figure of merit $ZT = S^2T/\rho(\kappa_l + \kappa_e)$, the power factor S^2/ρ has to be high. Unfortunately, the thermopower S and the electrical resistivity ρ are interrelated in an unfavorable way. Metallic samples with low ρ typically have low S and high electronic thermal conductivity κ_e. On the other hand, semiconducting samples with large S have too large ρ. Hence, the best ZT value for a compound can only be a compromise and has to be obtained by optimizing the charge carrier concentration, and thus the chemical composition.

Clathrates in the Ba-Ni-Ge system allow for controlled variation of the charge carrier concentration within the homogeneity range.[3,4] The compositions can be rationalized within a hypothetical Zintl phase $Ba_8Ge_{42}\square_4$, in which the vacancies (□) are successively filled by Ni atoms.[3] Depending on the Ni content, the phase shows a metal-to-insulator transition as well as a transition from *p*-type to *n*-type conduction.[3–5] To further explore the chemical composition and structural details and their influence on the physical properties, investigations of single crystals are needed.

EXPERIMENTAL PROCEDURES

Single-phase polycrystalline starting material for crystal growth was prepared in an argon-filled glove box (O_2, $H_2O < 1$ ppm) from the elements in a 8:4:42

(Received July 10, 2009; accepted June 16, 2010; published online August 19, 2010)

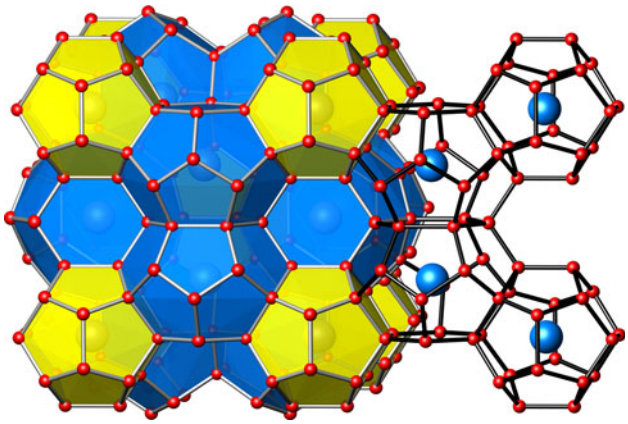

Fig. 1. Structure of type I clathrates with X_{20} cages (*yellow/light*) and X_{24} cages (*blue/dark*).

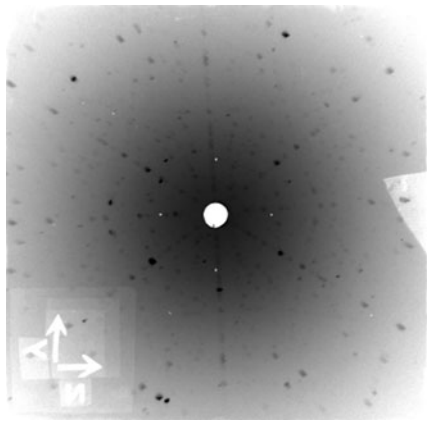

Fig. 3. Typical x-ray Laue back-reflection photograph of a crystal of $Ba_8Ni_{3.5}Ge_{42.1}\square_{0.4}$ showing the [011] orientation.

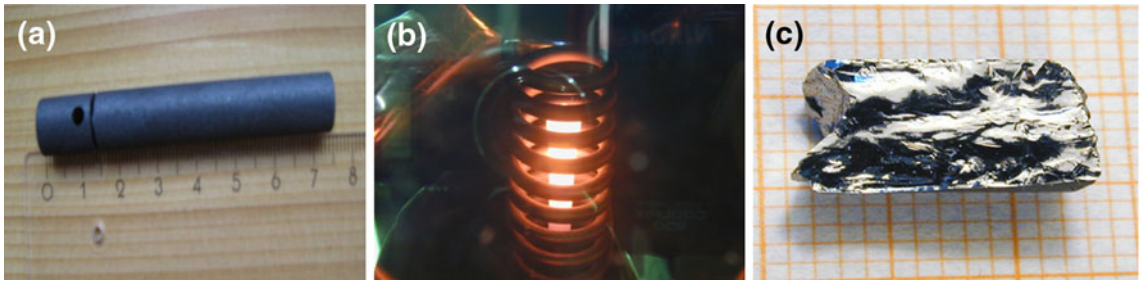

Fig. 2. Process steps of the crystal growth (see text).

ratio. Mixtures of crystalline Ba (Chempur, 99.9% metal basis), Ni foil (Chempur, 99.9% metal basis), and Ge pieces (Chempur, 99.9999%) were weighed in glassy-carbon crucibles (ø 12 mm, l = 12 mm, Sigradur G, HTW) and heated in an induction furnace (Hüttinger, 5 kW; coil ø 40 mm, length 35 mm, IR pyrometer, Maurer).

Differential thermal analysis (DTA) measurements showed that the material melts congruently and that single-crystal growth by the vertical Bridgman method with open graphite crucibles was possible. The polycrystalline starting material was put into a graphite crucible of approximately 8 mm diameter (Fig. 2a). The growth chamber was filled with Ar (~2 bar), and the crucible was heated by induction to 900°C during 1 h (Fig. 2b). The crucible was then slowly moved out of the radiofrequency (RF) coil, from the hot to the cold zone, at a speed of around 2 mm/h. A typical crystal grown by this technique is shown in Fig. 2c. The crystallinity of all samples was confirmed by Laue investigations. Various crystals were indexed and oriented[6] (Fig. 3).

A surface of the single crystal parallel to the growth direction was polished and investigated by energy-dispersive x-ray spectroscopy (EDXS), wavelength-dispersive x-ray spectroscopy (WDXS), and metallography. There is essentially no concentration gradient along the growth direction. The lattice parameter a = 10.680(1) Å was determined from powder diffraction[7] using LaB_6 as an internal standard. This is slightly larger than the value a = 10.676(1) Å given in Ref. 8 and much larger than the value a = 10.5179(4) Å given in Ref. 9, both for the nominal composition $Ba_8Ni_6Ge_{40}$.

In the clathrate I phase of the Ba-Ni-Ge system, Ge atoms, Ni atoms, and vacancies share the same crystallographic site. Therefore, the chemical composition cannot be independently refined from x-ray diffraction data.[3] For the structure refinement, the Ba:Ni ratio was taken from the WDXS result $Ba_{8.00(3)}Ni_{3.45(3)}Ge_{42.3(2)}$, obtained using Ba_6Ge_{25} and Ni as standards. Refinement of x-ray powder data using the Rietveld method resulted in the final composition of $Ba_8Ni_{3.5}Ge_{42.1}\square_{0.4}$.

RESULTS AND DISCUSSION

The electrical resistivity ρ increases with increasing temperature T, a sign of metallic conduction (Fig. 4). The high residual resistivity value, ρ(2 K) = 0.68 mΩ cm, as well as the low residual resistance ratio, RRR = R(300 K)/R(2 K) = 1.5, suggest classification of $Ba_8Ni_{3.5}Ge_{42.1}\square_{0.4}$ as a poor metal.

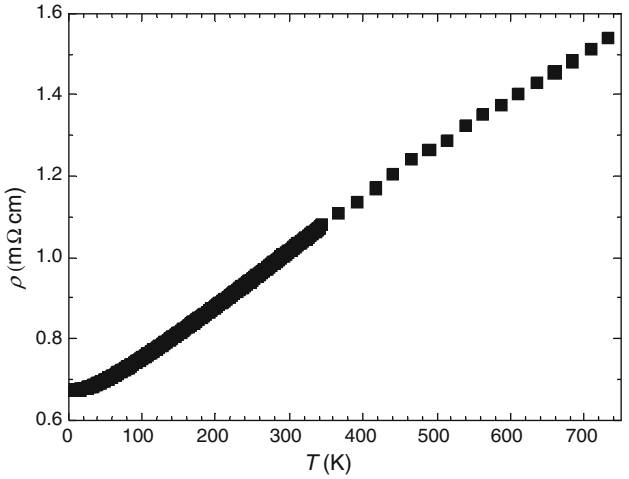

Fig. 4. Temperature dependence of the electrical resistivity, $\rho(T)$, of $Ba_8Ni_{3.5}Ge_{42.1}\square_{0.4}$.

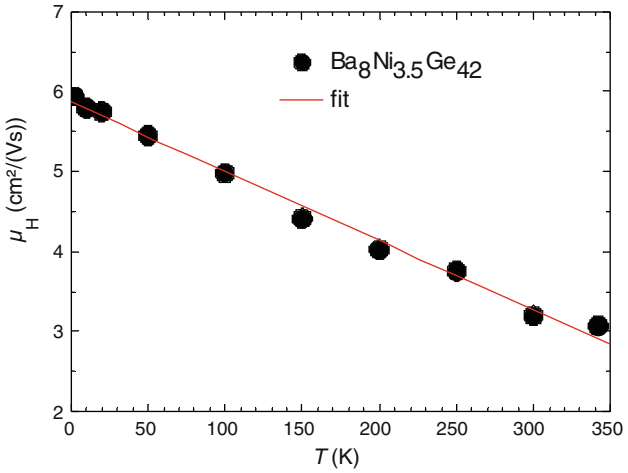

Fig. 6. Hall mobility, μ_H, versus temperature, T, of $Ba_8Ni_{3.5}Ge_{42.1}\square_{0.4}$. The line is a linear fit to the data.

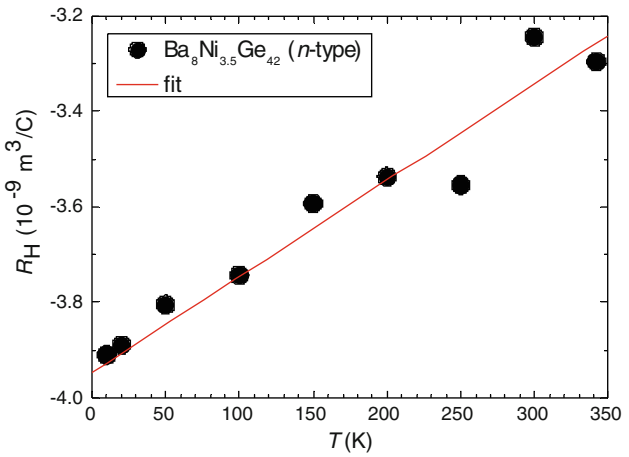

Fig. 5. Hall coefficient, R_H, versus temperature, T, of $Ba_8Ni_{3.5}Ge_{42.1}\square_{0.4}$. The line is a linear fit to the data.

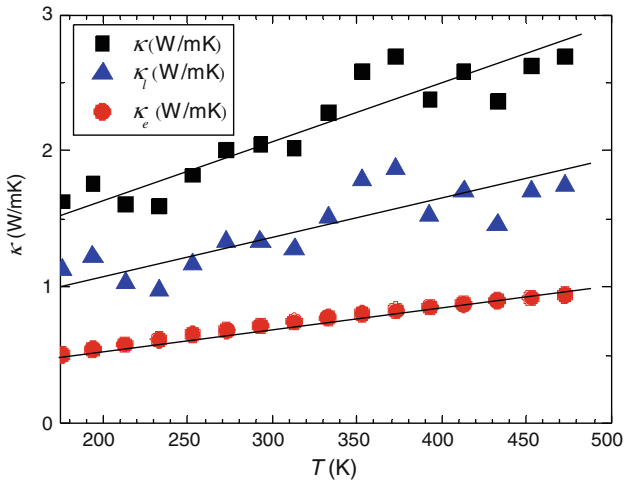

Fig. 7. Temperature dependence of thermal conductivity, $\kappa(T)$, of $Ba_8Ni_{3.5}Ge_{42.1}\square_{0.4}$. The lines are linear fits to the data.

The Hall coefficient R_H was measured in magnetic fields up to 9 T (Fig. 5). The charge carrier concentration calculated from $n = 1/(eR_H)$ is -1.9×10^{21} cm^{-3} at 300 K (2.3 e$^-$/unit cell). The dominant charge carries are electrons (n-type), in contrast to holes found in $Ba_8Ni_{6-x}Ge_{40+x}$ (x = 0 to 0.6).[5]

The Hall mobility, μ_H, decreases with increasing temperature (Fig. 6). Its room-temperature value, $\mu_H = 3.2$ cm^2 V^{-1} s^{-1}, fits well into the mobility–carrier concentration relation established for transition-metal clathrates by Johnsen et al.[4]

The thermal conductivity of $Ba_8Ni_{3.5}Ge_{42.1}\square_{0.4}$, κ, measured by the laser flash technique, increases with increasing temperature. At 300 K, it is similar to the value for $Ba_8Ga_{16}Ge_{30}$ but higher than the value for $Sr_8Ga_{16}Ge_{30}$.[10,11] The lattice thermal conductivity, κ_l, was calculated by using the Wiedemann–Franz law for the electronic contribution κ_e, $\kappa_l = \kappa - \kappa_e = \kappa - LT/\rho$, with the Lorenz number $L = 2.44 \times 10^{-8}$ WΩ/K^2. As seen in Fig. 7, both κ_e and κ_l contribute significantly to the total thermal conductivity κ.

The thermopower, measured by a four-point steady-state technique, is, with an absolute value of 55 μV/K at 300 K (Fig. 8), within the range found for $Ba_8Ga_{16-x}Ge_{30+x}$ (24 μV/K[10] to 120 μV/K[12]).

The temperature-dependent dimensionless thermoelectric figure of merit $ZT(T)$ is shown in Fig. 9. Using a linear extrapolation of the thermal conductivity data to higher temperatures, it is estimated to reach a maximum of $ZT_{max} \approx 0.2$ at 680 K. This is higher than for n-type $Ba_8Ga_6Ge_{40}$ ($ZT_{max} \approx 0.02$ at 300 K)[12] but lower than for n-type α- and β-$Eu_8Ga_{16}Ge_{30}$ ($ZT_{max} \approx 0.4$ at 400 K).[13] For thermoelectric applications, the Seebeck coefficient and the resistivity need to be improved by optimizing the Ni content and thus the carrier concentration.

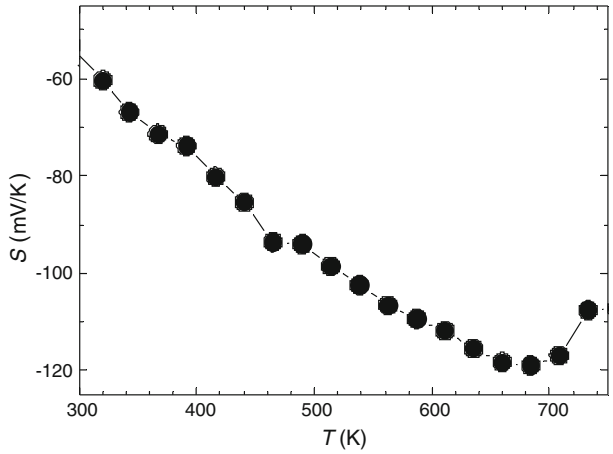

Fig. 8. Temperature dependence of the thermopower, $S(T)$, of $Ba_8Ni_{3.5}Ge_{42.1}\square_{0.4}$.

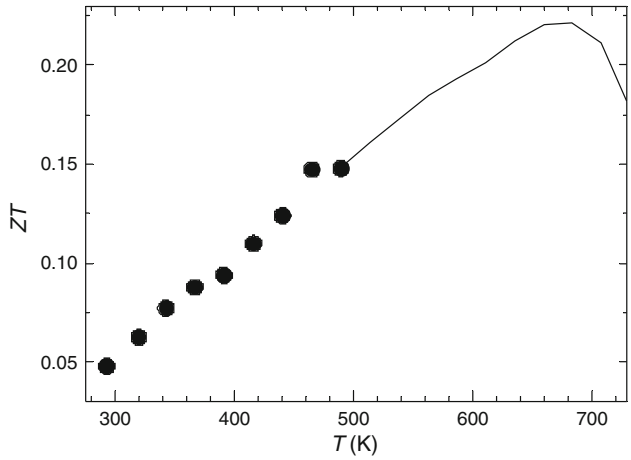

Fig. 9. Thermoelectric figure of merit, ZT, versus temperature, T, of $Ba_8Ni_{3.5}Ge_{42.1}\square_{0.4}$. The line is obtained by linear extrapolation of $\kappa(T)$ (Fig. 7) to higher temperatures.

CONCLUSIONS

$Ba_8Ni_{3.5}Ge_{42.1}\square_{0.4}$ single crystals were grown by the Bridgman method. Structural and transport properties were investigated. $Ba_8Ni_{3.5}Ge_{42.1}\square_{0.4}$ is an n-type thermoelectric material with $ZT \approx 0.2$ at 680 K. For thermoelectric applications, further optimization of the charge carrier concentration via variation of the Ni content is necessary.

ACKNOWLEDGEMENT

Financial support from the EU FP6 NoE Complex Metallic Alloys is gratefully acknowledged.

REFERENCES

1. J.L. Cohn, G.S. Nolas, V. Fessatidis, T.H. Metcalf, and G.A. Slack, *Phys. Rev. Lett.* 82, 779 (1999).
2. M. Christensen, A. Abrahamsen, N. Christensen, F. Juranyi, N. Andersen, K. Lefmann, J. Andreasson, C. Bahl, and B. Iversen, *Nature Mater.* 7, 811 (2008).
3. M. Baitinger, U. Aydemir, B. Böhme, H. Borrmann U. Burkhardt, W. Carrillo-Cabrera, A. Guloy, F. Haarmann, W. Jung, K. Kovnir, L.N.T. Kim, R. Ramlau, W. Schnelle, U. Schwarz, A. Shevelkov, Z. Tang, J. Vezemchuk, J. Zaikina, and Yu. Grin, *In Scientific Report 2006/2008* (Max Planck Institute for Chemical Physics of Solids, Dresden, 2009), p. 134.
4. S. Johnsen, A. Bentien, G.K.H. Madsen, M. Nygren, and B.B. Iversen, *Phys. Rev. B* 76, 245126 (2007).
5. A. Bentien, S. Johsen, and B.B. Iversen, *Phys. Rev. B* 73, 094301 (2006).
6. Software Orient Express 3.4, http://www.ccp14.ac.uk/ccp/web-mirrors/lmgp-laugier-bochu.
7. L.G. Akselrud, P.Y. Zavalli, Yu. Grin, V.K. Pecharsky, B. Baumgartner, and E. Wölfel, *Mater. Sci. Forum* 335, 133 (1993).
8. G. Cordier and P. Woll, *J. Less-Common Met.* 169, 291 (1991).
9. H. Zhang, J.T. Zhao, M.B. Tang, Z.Y. Man, H.H. Chen, and X.X. Yang, *J. Phys. Chem. Solids* 70, 312 (2009).
10. N.L. Okamoto, K. Kishida, K. Tanaka, and H. Inui, *J. Appl. Phys.* 101, 113525 (2007).
11. L. Qui, I.P. Swainson, G.S. Nolas, and M.A. White, *Phys. Rev. B* 70, 035208 (2004).
12. N.L. Okamoto, K. Kishida, K. Tanaka, and H. Inui, *J. Appl. Phys.* 100, 073504 (2006).
13. A. Bentien, V. Pacheco, S. Paschen, Yu. Grin, and F. Steglich, *Phys. Rev. B* 71, 165205 (2005).